

OPEN

Lupus-like Disease in $Fc\gamma RIIB^{-/-}$ Mice Induces Osteopenia

Peerapat Visitchanakun^{1,2}, Worasit Saiworn^{1,2}, Prapaporn Jongwattanapisan³, Asada Leelahavanichkul⁴, Prapaporn Pisitkun⁵ & Sutada Lotinun^{1,2*}

Osteoporotic fracture is a major cause of morbidity in patients with systemic lupus erythematosus (SLE). Mice lacking Fc gamma receptor IIb ($Fc\gamma RIIB$) spontaneously develop lupus-like disease or SLE at 6-month-old. The aim of this study was to investigate whether $Fc\gamma RIIB$ deletion induces osteopenia. μ CT analysis indicated that deleting $Fc\gamma RIIB$ did not affect cancellous bone microarchitecture in 3-month-old mice in which SLE had not yet developed. However, 6- and 10-month-old $Fc\gamma RIIB^{-/-}$ males that developed an SLE-like phenotype were osteopenic and $Fc\gamma RIIB$ deletion resulted in decreased cancellous bone volume. Histomorphometry confirmed a significant decrease in cancellous bone volume in 6- and 10-month-old $Fc\gamma RIIB^{-/-}$ males. The osteoclast number was increased without any change in osteoblast number. *In vitro* assays indicated that deleting $Fc\gamma RIIB$ increased osteoclast differentiation while alkaline phosphatase activity and mineralization were unaltered. These changes were associated with increases in steady-state mRNA levels for the osteoclast marker genes *Trap* and *Ctsk*. Moreover, $Fc\gamma RIIB^{-/-}$ mice had higher level of serum $TNF\alpha$, a proinflammatory cytokine. A soluble $TNF\alpha$ receptor, etanercept, prevented cancellous bone loss in $Fc\gamma RIIB^{-/-}$ mice. Our results indicate that $Fc\gamma RIIB$ indirectly regulates cancellous bone homeostasis following SLE development. $Fc\gamma RIIB$ deletion induces inflammatory bone loss due to increased $TNF\alpha$ -mediated bone resorption without any change in bone formation in mice with SLE-like syndrome.

Systemic autoimmune diseases with complex multifactorial etiologies including systemic lupus erythematosus (SLE) are associated with low bone mass and fracture. SLE is more common in African American, Hispanic, and Asian compared to Caucasian women. Patients with SLE are at an increased risk for osteoporosis for several reasons. Systemic inflammation, metabolic factors, serological factors, hormonal factors, genetic factors and medication can increase bone loss in these patients¹. Glucocorticoids commonly prescribed for SLE because of their rapid and broad spectrum in suppressing disease activity and preventing irreversible organ damage can trigger significant bone loss. However, it has been shown that SLE patients on long-term glucocorticoids and those not on glucocorticoids have significantly decreased BMD compared to healthy individuals². There was no difference in BMD between the patients taking glucocorticoids and no glucocorticoids. Therefore, SLE itself or other factors may have deleterious effects on bone mass.

Osteoimmunology studies indicate a complex interplay between the immune and skeleton systems. Although osteoporosis and high fracture risk are well-known consequences of SLE, the cause of low bone mass in SLE patients remains unclear. The deposition of immune complexes (ICs) plays a major role in the pathogenesis of SLE. Receptors for the Fc domain of IgG ($Fc\gamma$ Rs) are important for IC clearance. In SLE, impaired Fc-mediated IC clearance initiates the release of inflammatory mediators and influx of inflammatory cells. Four classes of $Fc\gamma$ R, $Fc\gamma RI$, $Fc\gamma RII$, $Fc\gamma RIII$ and $Fc\gamma RIV$ have been identified in mice³. $Fc\gamma RIIB$, a negative regulator of IC-triggered activation, is associated with susceptibility to autoimmune disease, particularly SLE^{4,5}. This inhibitory receptor functions to suppress the development of autoimmunity by regulating B-cell responses and effector cell activation⁶. The abnormal low expression of B-cell $Fc\gamma RIIB$ in SLE leads to inadequate suppression of autoantigen-mediated B-cell receptor activation. $Fc\gamma RIIB$ deficient mice had exacerbated autoimmune symptoms, and a partial restoration of functional $Fc\gamma RIIB$ expression on B cells was sufficient to rescue mice from developing lupus-like disease^{7,8}.

¹Department of Physiology, Faculty of Dentistry, Chulalongkorn University, Bangkok, Thailand. ²Skeletal Disorders Research Unit, Faculty of Dentistry, Chulalongkorn University, Bangkok, Thailand. ³Department of Veterinary Medicine, Faculty of Veterinary Science, Chulalongkorn University, Bangkok, Thailand. ⁴Division of Immunology, Department of Microbiology, Faculty of Medicine, Chulalongkorn University, Bangkok, Thailand. ⁵Division of Allergy, Immunology, and Rheumatology, Department of Medicine, Faculty of Medicine, Ramathibodi Hospital, Mahidol University, Bangkok, Thailand. *email: sutada.l@chula.ac.th

The involvement of Fc γ R in bone homeostasis has been studied. Activating, Fc γ RI, Fc γ RIIA, Fc γ RIII and Fc γ RIV, and inhibitory Fc γ R, Fc γ RIIB, are expressed on osteoclasts⁹. Binding of ICs that contain IgG to Fc γ R results in the activation of macrophages in synovial and cartilage layers. The activating Fc γ R directly induces severe cartilage destruction, but not bone erosion¹⁰. Arthritic mice lacking Fc γ RI/II/III demonstrated an increased level of joint inflammation. It was concluded that the absence of Fc γ RI/II/III drives joint inflammation, thereby indirectly causing bone resorption. Immunostaining revealed that the amount of RANKL-positive inflammatory cells was higher in the exudate of arthritic knee joints of Fc γ RI/II/III^{-/-} mice compared to controls. Fc γ RIV deletion in osteoclasts in a K/BxN serum transfer arthritis model decreased osteoclast differentiation without reducing the clinical signs of arthritis⁹. H-2^b mice deficient in Fc γ RIIB were susceptible to collagen-induced arthritis after immunization with native type II collagen¹¹.

Our previous study indicated that mice with an Fc γ RIIB deletion resulted in SLE active disease at 6 months old. The Fc γ RIIB^{-/-} mice had cortical bone loss and decreased mechanical properties at 6 and 10 months old after the development of SLE or lupus disease¹². The purpose of the present study was to determine the mechanism by which the absence of Fc γ RIIB affected cancellous bone turnover. Similar to the cortical bone phenotype, no change in cancellous bone volume was observed in 3-month-old Fc γ RIIB^{-/-} mice. However, 6 and 10 months old Fc γ RIIB^{-/-} males had cancellous bone loss due to elevated bone resorption without any change in bone formation. Deletion of Fc γ RIIB decreased cancellous bone volume in 10-, but not 6-month-old female knockouts. Serum TNF α level was increased in Fc γ RIIB knockouts. Etanercept, a TNF α inhibitor, increased cancellous bone volume and trabecular thickness in Fc γ RIIB^{-/-} mice. These data suggested that the absence of Fc γ RIIB induced inflammation and cancellous osteopenia in mice with lupus-like syndrome.

Results

Fc γ RIIB deletion did not affect cancellous bone in young adult mice. Our previous study indicated that 3-month-old Fc γ RIIB^{-/-} mice have a normal cortical bone phenotype¹². To determine whether Fc γ RIIB deletion affected cancellous bone homeostasis in 3-month-old mice, we examine the skeletal phenotype of 3-month-old Fc γ RIIB^{-/-} and Fc γ RIIB^{+/-} males and their WT controls. μ CT analysis revealed no difference in cancellous bone volume, trabecular thickness, trabecular number (data not shown), trabecular separation, or SMI between groups (Fig. 1A,B). Mice deficient in Fc γ RIIB on a C57BL/6 background developed a lupus-like autoimmunity at 6 months of age as indicated by an increased serum level of anti-dsDNA antibody and spleen B220^{low}CD138⁺ plasma cells¹². Therefore, our results indicated that Fc γ RIIB deletion did not affect skeletal homeostasis at 3 months of age when SLE disease was not active.

6- and 10-month-old Fc γ RIIB^{-/-} males had low cancellous bone volume due to increased osteoclast number. We examined whether the older Fc γ RIIB^{-/-} mice with active SLE had decreased cancellous bone. The μ CT images and analysis of the proximal tibiae in 6- and 10-month-old Fc γ RIIB^{-/-} males are shown in Fig. 1A,B, respectively. Cancellous bone volume was decreased by 19% and structural model index was increased by 33% in 6-month-old Fc γ RIIB^{-/-} males. However, trabecular thickness, trabecular number (data not shown), and trabecular separation were not changed. Ten months old Fc γ RIIB^{-/-} males had decreased cancellous bone volume and trabecular thickness by 36% and 28%, respectively. Structural model index was decreased by 17%.

Histomorphometric analysis of the femur metaphysis showed a significant decrease in cancellous bone volume at 6 months of age in Fc γ RIIB^{-/-} males (Table 1). Trabecular thickness was decreased in knockouts. However, bone formation parameters, including mineral apposition rate, mineralizing surface, bone formation rate, osteoblast number, osteoid volume and osteoid thickness were not altered (Table 1). In contrast, osteoclast surface per bone surface, osteoclast number per tissue area and osteoclast number per bone perimeter were markedly increased at 6 months of age. Similar to the μ CT analysis, the skeletal phenotype was more severe in older mice. Fc γ RIIB deletion dramatically decreased cancellous bone volume by 48%. Trabecular thickness, and trabecular number were decreased whereas trabecular separation was increased. Osteoclast surface per bone surface and osteoclast number per bone perimeter were increased compared to controls, leading to bone loss in Fc γ RIIB^{-/-} mice. There was no statistical significant difference between Fc γ RIIB^{-/-} and control mice in all indices of bone formation at 10 months of age.

Fc γ RIIB^{-/-} females were osteopenic at 10 months old. To compare the skeletal phenotype observed in females to males, we performed μ CT analysis in 6 and 10 months old Fc γ RIIB^{-/-} females. Fc γ RIIB^{-/-} females had a normal cancellous bone phenotype at 6 months of age (Fig. 2A,B). The μ CT analysis indicated that cancellous bone microarchitecture did not change in 6-month-old Fc γ RIIB^{-/-} females. There was no change in cancellous bone volume, trabecular thickness, trabecular number (data not shown), trabecular separation, or SMI. However, 10-month-old Fc γ RIIB^{-/-} females were osteopenic (Fig. 2A,B). Cancellous bone volume was reduced due to decreased trabecular thickness, however, trabecular number (data not shown), and trabecular separation did not change. The higher SMI was observed in Fc γ RIIB^{-/-} females compared to WT controls.

Increased bone resorption in Fc γ RIIB^{-/-} mice was due to increased osteoclastogenesis. Histomorphometry indicated that Fc γ RIIB deletion led to increased osteoclast number without any change in osteoblast number in 6 and 10 months old males. To confirm that this deletion did not affect bone formation, we performed an *in vitro* assay using primary osteoblasts derived from long bones. ALP and mineralized bone nodules were similar in osteoblasts derived from Fc γ RIIB^{-/-} mice and their control littermates, indicating that deletion of Fc γ RIIB did not affect osteoblast differentiation or mineralization (Fig. 3A).

We determined whether the increased osteoclast number in Fc γ RIIB^{-/-} mice led to cancellous bone loss. An *in vitro* osteoclast differentiation assay was performed. Consistent with the increased bone resorption observed *in vivo*, deletion of Fc γ RIIB increased TRAP positive osteoclasts derived from bone marrow macrophages (BMMs)

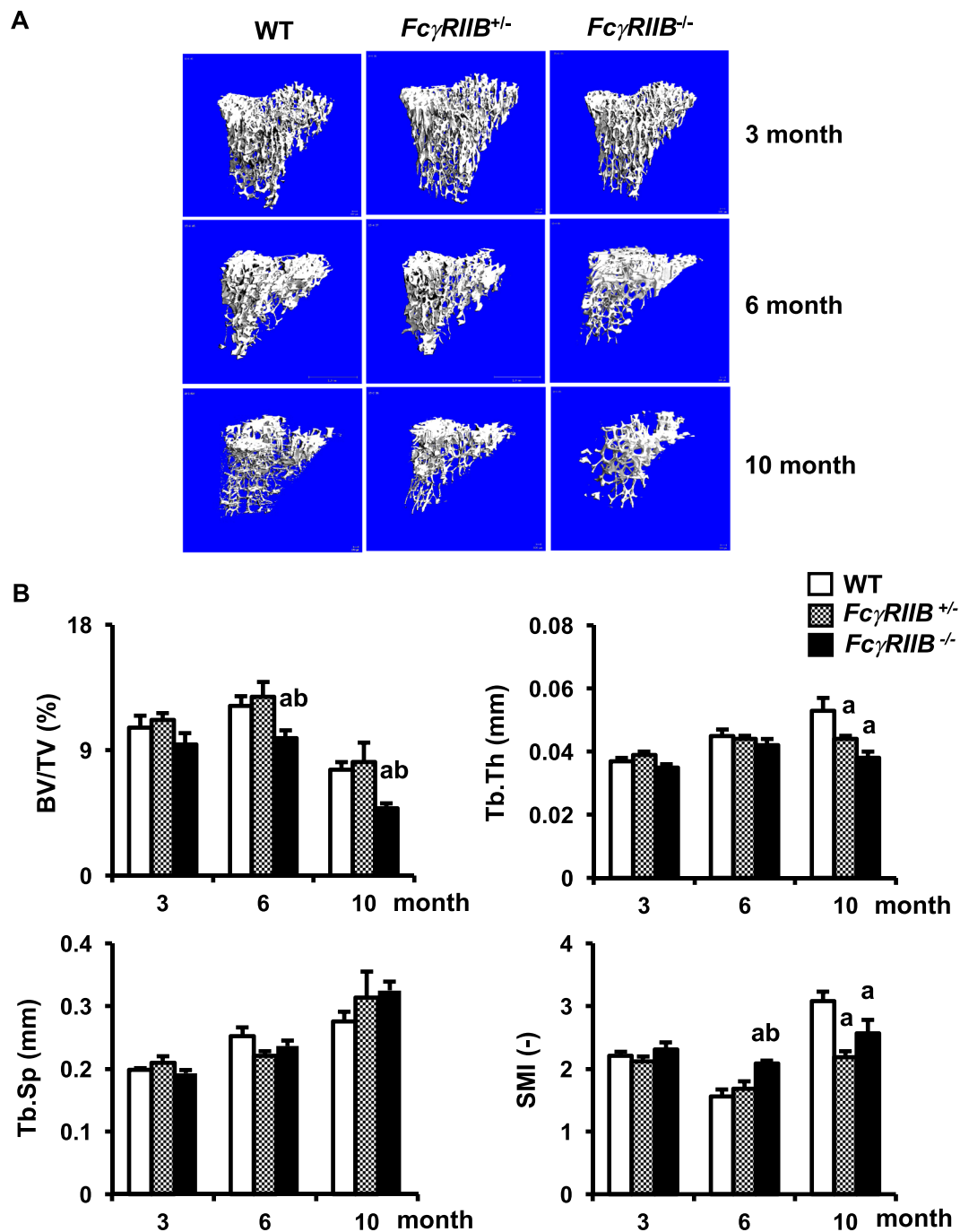


Figure 1. Absence of *FcγRIIB* induces cancellous bone loss in 6- and 10-month-old males. **(A)** Representative μ CT images of the tibial cancellous bone from 3-, 6- and 10-month-old *FcγRIIB*^{+/-} and *FcγRIIB*^{-/-} males compared to their WT controls. **(B)** μ CT analysis of the proximal tibial metaphysis. Results are mean \pm SEM. ^a $p < 0.05$ versus corresponding WT controls, and ^b $p < 0.05$ versus corresponding *FcγRIIB*^{+/-} mice. BV/TV; bone volume per tissue volume, Tb.Th; trabecular thickness, Tb.Sp; trabecular separation and SMI; structural model index.

of both 6- and 10-month-old mice compared to WT controls (Fig. 3B). These data revealed the major role of *FcγRIIB* in osteoclast differentiation subsequent to SLE development.

To investigate whether the presence of *FcγRIIB*^{-/-} osteoblasts had a role in modulating osteoclast function, osteoblasts derived from *FcγRIIB*^{-/-} mice and WT controls were co-cultured with BMMs derived from either *FcγRIIB*^{-/-} mice or WT controls. Osteoclast number was increased when BMMs from *FcγRIIB*^{-/-} mice were co-cultured with osteoblasts from either *FcγRIIB*^{-/-} mice or WT (Fig. 4). We observed similar number of osteoclasts generated in co-cultures of WT BMMs with either *FcγRIIB*^{-/-} or WT osteoblasts. These data revealed that deletion of *FcγRIIB* in BMMs stimulated osteoclast differentiation.

Parameters	6-month-old		10-month-old	
	WT	<i>FcγRIIB</i> ^{-/-}	WT	<i>FcγRIIB</i> ^{-/-}
	(n = 7)	(n = 6)	(n = 7)	(n = 6)
BV/TV (%)	11.58 ± 1.17	7.76 ± 1.06*	8.66 ± 1.00	4.47 ± 0.32*
Tb.Th (μm)	44.93 ± 3.80	33.96 ± 2.09*	41.86 ± 3.10	29.62 ± 1.73*
Tb.N (/mm)	2.60 ± 0.22	2.42 ± 0.27	2.08 ± 0.17	1.51 ± 0.08*
Tb.Sp (μm)	356 ± 32	421 ± 67	462 ± 45	640 ± 32*
MS/BS (%)	20.64 ± 2.34	22.81 ± 2.54	14.88 ± 2.58	19.78 ± 2.78
MAR (μm/day)	1.14 ± 0.06	1.02 ± 0.04	1.28 ± 0.20	1.29 ± 0.40
BFR/BS (μm ³ /μm ² /year)	85 ± 11	85 ± 11	70 ± 19	79 ± 11
BFR/BV (%/year)	415 ± 54	507 ± 73	357 ± 77	502 ± 54
BFR/TV (%/year)	54 ± 7	50 ± 9	27 ± 8	26 ± 4
Ob.S/BS (%)	7.10 ± 1.70	5.58 ± 1.42	2.16 ± 0.64	1.81 ± 0.61
N.Ob/T.Ar (/mm ²)	31.03 ± 8.95	20.29 ± 5.70	6.61 ± 2.08	4.23 ± 1.30
N.Ob/B.Pm (/mm)	5.65 ± 1.27	4.33 ± 1.22	1.63 ± 0.55	1.47 ± 0.49
OV/TV (%)	0.023 ± 0.007	0.018 ± 0.008	0.006 ± 0.006	0.005 ± 0.002
OS/BS (%)	1.38 ± 0.39	1.10 ± 0.49	0.44 ± 0.39	0.54 ± 0.27
O.Th (μm)	2.18 ± 0.57	2.36 ± 0.77	0.95 ± 0.64	1.48 ± 0.68
Oc.S/BS (%)	0.31 ± 0.09	1.35 ± 0.47*	0.73 ± 0.23	1.87 ± 0.39*
N.Oc/T.Ar (/mm ²)	0.58 ± 0.19	2.43 ± 0.81*	0.94 ± 0.30	1.67 ± 0.33
N.Oc/B.Pm (/mm)	0.11 ± 0.03	0.50 ± 0.17*	0.23 ± 0.07	0.54 ± 0.08*
ES/BS (%)	0.13 ± 0.08	0.73 ± 0.30	0.43 ± 0.16	0.85 ± 0.25

Table 1. Histomorphometric analysis of femurs from 6- and 10-month-old *FcγRIIB*^{-/-} males and their control littermates. Results are mean ± SEM. **p* < 0.05 compared to corresponding WT controls, unpaired *t*-test. BV/TV; bone volume per tissue volume, Tb.Th; trabecular thickness, Tb.N; trabecular number, Tb.Sp; trabecular separation, MS/BS; mineralizing surface per bone surface, MAR; mineral apposition rate, BFR/BS; bone formation rate per bone surface, BFR/BV; bone formation rate per bone volume, BFR/TV; bone formation rate per tissue volume, Ob.S/BS; osteoblast surface per bone surface, N.Ob/T.Ar; osteoblast number per tissue area, N.Ob/B.Pm; osteoblast number per bone perimeter, OV/TV; osteoid volume per tissue volume, OS/BS; osteoid surface per bone surface, O.Th; osteoid thickness, Oc.S/BS; osteoclast surface per bone surface, N.Oc/T.Ar; osteoclast number per tissue area, N.Oc/B.Pm; osteoclast number per bone perimeter, and ES/BS; eroded surface per bone surface.

***FcγRIIB* regulates the expression of bone resorption genes.** Deletion of *FcγRIIB* increased bone resorption without any effect on bone formation in both *in vivo* and *in vitro*. The skeletal phenotype was more pronounced in 10-month-old *FcγRIIB*^{-/-} males. We then selected these mice to determine whether *FcγRIIB* deletion affected any gene expression. qPCR analysis revealed that osteoblast marker genes, including *Alp*, *type I collagen*, *Osx*, *osteopontin*, *osteocalcin*, and *Sost* expression did not alter (Fig. 5). In contrast, deletion of *FcγRIIB* increased the mRNA levels for osteoclast marker genes, including *Trap*, and *Ctsk*. However, the *RANKL/OPG* ratio, *M-CSF*, *Nfatc1*, *Tnfα*, *c-Fms* and *IFNγ* mRNA levels were not affected in *FcγRIIB*^{-/-} mice.

***FcγRIIB*^{-/-} mice produced higher TNFα serum level.** To investigate whether the absence of *FcγRIIB* increased inflammation, the serum levels of proinflammatory cytokines including TNFα, and IL-6 were determined in 6 and 10 months old *FcγRIIB*^{-/-} males and WT controls. *FcγRIIB* deletion increased the serum level of TNFα, whereas that of IL-6 was not affected (Fig. 6). The higher TNFα serum level was more pronounced in 10-month-old *FcγRIIB*^{-/-} mice. Serum IL-10, a potent anti-inflammatory cytokine, was also measured. We did not observe any change in the serum level of IL-10. We also determined whether the serum TNFα level was altered in 3 months old *FcγRIIB*^{-/-} males. There was no change in the serum TNFα level in 3-month-old *FcγRIIB*^{-/-} males compared to WT (5.52 ± 0.16 vs 5.98 ± 0.43 pg/ml). Our data indicated that the serum level of TNFα was increased following SLE development.

TNFα antagonist prevents cancellous bone loss in *FcγRIIB*^{-/-} mice. We examined whether TNFα is a key factor that induced cancellous bone loss in *FcγRIIB*^{-/-} mice. Etanercept, a recombinant human soluble fusion protein of TNFα type II receptor linked to Fc portion of IgG1, was used to block TNFα function. μCT data confirmed that 6-month-old *FcγRIIB*^{-/-} mice were osteopenic as mentioned earlier (Fig. 7). Inhibition of TNFα increased cancellous bone volume by 49 and 139% in WT and *FcγRIIB*^{-/-} mice, respectively. SMI was decreased by etanercept treatment in both *FcγRIIB*^{-/-} mice and WT controls. *FcγRIIB*^{-/-} mice treated with etanercept had increased trabecular thickness with a concomitant decrease in trabecular separation. Two-way ANOVA indicated no interaction between *FcγRIIB* deletion and etanercept on any parameter. These findings confirmed that TNFα mediated osteopenia in *FcγRIIB*^{-/-} mice and that blocking TNFα prevented cancellous bone loss.

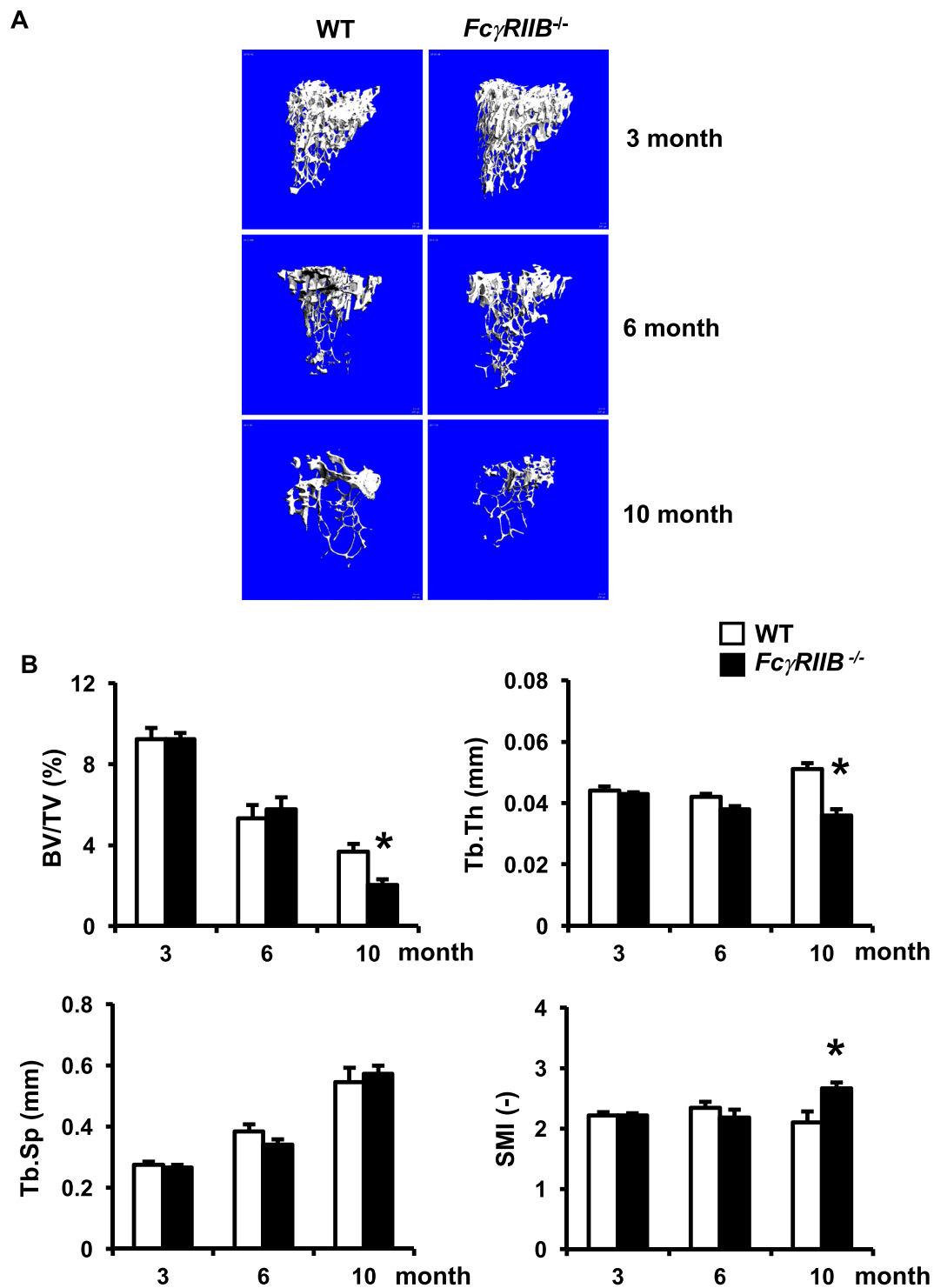


Figure 2. *Fc γ RIIB* deletion decreases cancellous bone volume in 10 months old females. (A) Representative μ CT images of the tibial cancellous bone from 3-, 6- and 10-month-old *Fc γ RIIB*^{-/-} females and WT controls. (B) μ CT analysis of the proximal tibial metaphysis. Results are mean \pm SEM. * p < 0.05 versus corresponding WT controls. BV/TV; bone volume per tissue volume, Tb.Th; trabecular thickness, Tb.Sp; trabecular separation and SMI; structural model index.

Discussion

SLE is an autoimmune disease characterized by B-cell hyperactivity and B-cell receptor signaling abnormalities. SLE patients have a high prevalence of osteoporotic fracture leading to increased morbidity. The role of *Fc γ RIIB* in SLE-associated bone loss is not completely understood. In this study, we determined whether deleting

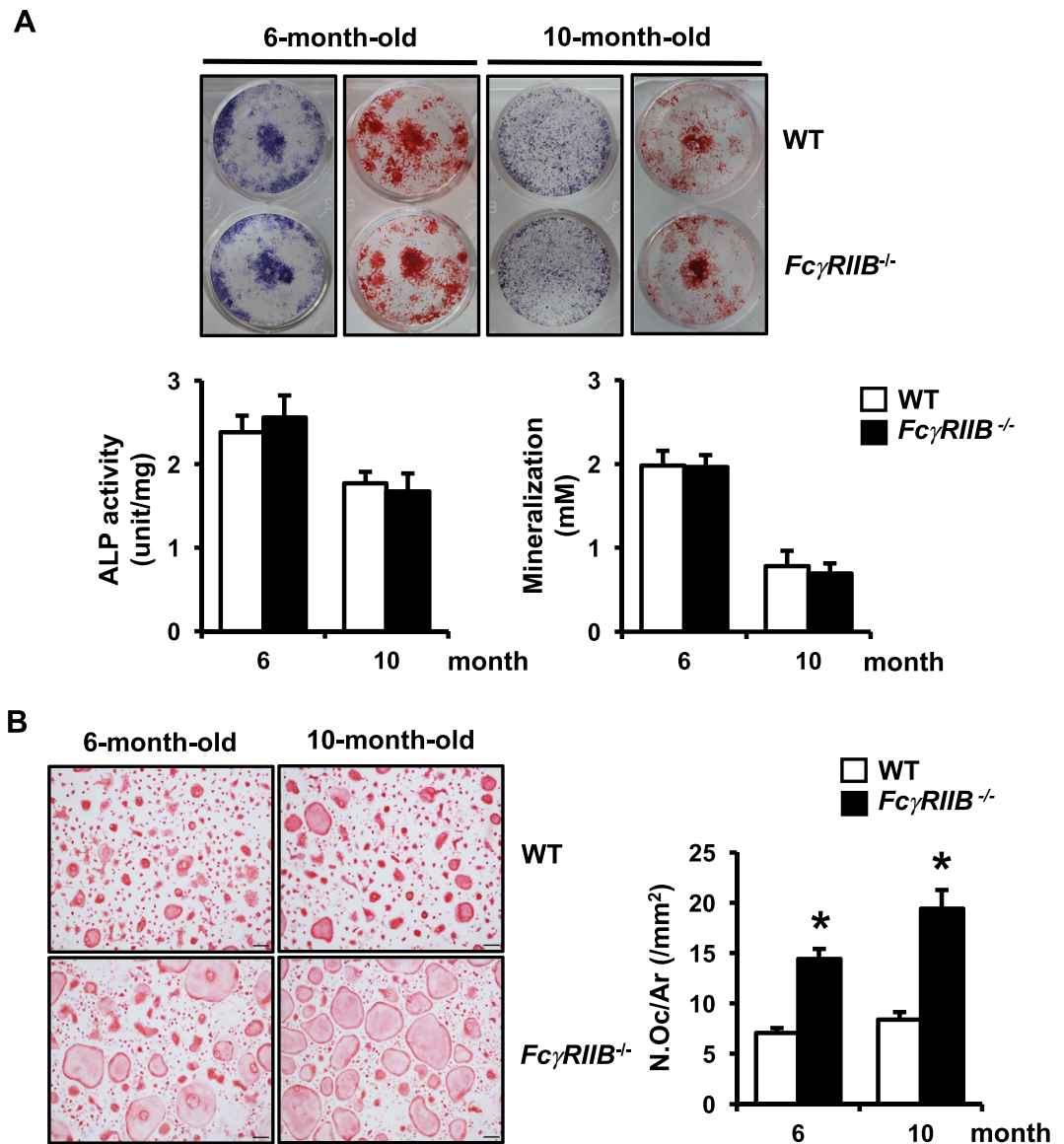


Figure 3. *FcγRIIB* deletion increases osteoclast, but not osteoblast differentiation. (A) ALP (left) and mineralized bone nodule (right) in osteoblasts derived from long bones of 6- and 10-month-old *FcγRIIB*^{-/-} males and WT controls. ALP activity (unit/mg) and mineralization or alizarin red concentration (mM) were quantified. (B) *FcγRIIB*^{-/-} and WT osteoclasts were generated on glass coverslips in the presence of M-CSF and RANKL (left). TRAP-positive spreading osteoclasts containing more than 5 nuclei per area were quantified by OsteoMeasure software, (OsteoMetrics, right). Results are mean ± SEM. **p* < 0.05 versus corresponding WT controls. ALP; alkaline phosphatase, N.Oc; osteoclast number and Ar; area. Scale bar: 100 μm.

FcγRIIB affected cancellous bone phenotype. We found that cancellous bone volume was similar in 3-month-old *FcγRIIB*^{-/-} mice compared to WT controls. However, *FcγRIIB* deletion reduced cancellous bone volume at 6 and 10 months old in males. The cancellous osteopenia was associated with increased osteoclast number without any change in osteoblast number. The expressions of *Trap* and *Ctsk*, osteoclast marker genes, was upregulated in knockouts. Female *FcγRIIB*^{-/-} mice had decreased cancellous bone volume at 10, but not 6 months old. Serum TNF-α level, a proinflammatory cytokine, was increased in knockouts. Blocking TNF-α increased cancellous bone volume. Our data suggest that the absence of *FcγRIIB* results in cancellous bone loss due to inflammation-induced osteoclastic bone resorption in a murine model of spontaneous SLE-like syndrome.

The causes of bone loss in SLE are multifactorial, involving factors intrinsic to the disease itself, adverse effects of medication, and genetic factors. Moreover, proteinuria and renal dysfunction may aggravate vitamin D insufficiency, leading to bone loss in lupus nephritis patients. Low bone mass has an early onset in these patients, most likely due to systemic inflammation-induced increased osteoclastic bone resorption and reduced osteoblastic bone formation. Increased proinflammatory cytokines, including TNFα, IL-1, IL-6, and IL-17 levels might increase the production of RANKL¹³. In addition, activated synovial T cells and fibroblasts express RANKL and

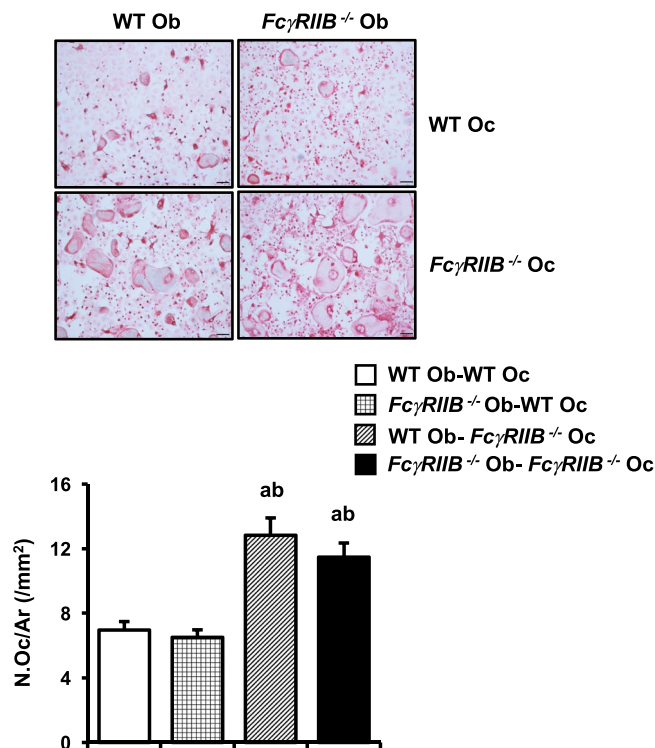


Figure 4. *FcγRIIB*^{-/-} osteoblasts had no effect on osteoclast differentiation. TRAP-positive spreading osteoclasts containing more than 5 nuclei per area from co-culture of either WT or *FcγRIIB*^{-/-} osteoblasts with WT or *FcγRIIB*^{-/-} BMMs. Results are mean ± SEM. ^a*p* < 0.05 versus WT Ob-WT Oc, and ^b*p* < 0.05 versus *FcγRIIB*^{-/-} Ob-WT Oc. Ob; osteoblasts, Oc; osteoclasts, N.Oc; osteoclast number and Ar; area. Scale bar: 100 μm.

TNFα to stimulate osteoclast differentiation during inflammation. The inhibition of the BMP/Smad pathway suppresses osteoblast differentiation through activated NF-κB signaling in SLE patients¹⁴.

Glucocorticoid use is a well-known risk factor for osteoporosis and fracture. However, glucocorticoid-induced osteoporosis in patients with SLE is still controversial. It has been reported that patients recently diagnosed with SLE without glucocorticoid treatment have decreased BMD compared to age-matched healthy individuals². The reduction of BMD is related to decreased serum osteocalcin and increased urinary pyridinoline, suggesting that the disease itself independent of glucocorticoid treatment may lead to bone loss¹⁵. These findings suggest that glucocorticoids are not the only mechanism responsible for low bone mass in patients with SLE.

Genetic factors contribute to SLE susceptibility and presumably have an important role in determining the etiology of the disease. *FcγR* regulates autoantibody and IC-induced inflammation. *FcγRIIB* is expressed on B-cells, mast cells, dendritic cells, neutrophils, macrophages, and osteoclasts^{9,16}. Decreased expression of *FcγRIIB* on germinal center B-cells was associated with strain-specific susceptibility to autoimmune disease. *FcγRIIB*^{-/-} mice on the C57BL/6 background spontaneously developed hypergammaglobulinemia, autoimmune glomerulonephritis and IC-mediated SLE-like disease⁷. In contrast, BALB/c mice deficient in *FcγRIIB* did not develop autoimmunity. This finding confirmed our previous study where *FcγRIIB*^{-/-} mice on the C57BL/6 background developed SLE at 6 months of age¹². The serum anti-dsDNA antibody levels and antibody-secreting B220^{low}CD138⁺ plasma cells, markers for SLE, were increased in 6-, but not 3-month-old *FcγRIIB*^{-/-} mice compared to WT controls. *FcγRIIB*-expressing retrovirus restored tolerance and prevented autoimmune disease in *FcγRIIB*^{-/-} mice⁸. The inhibitory role of *FcγRIIB* in the development of autoimmunity is supported by the evidence of SLE-associated *FcγRIIB* polymorphism in human¹⁷. In contrast, genetically deleting the activating *FcγRs* did not develop spontaneous autoimmune diseases in mice¹⁸. In addition, *FcγR* deletion did not have any effect on cancellous bone volume and osteoclast number¹⁹.

Despite extensive studies, genetic factors contributing to the increased bone loss in patients with SLE were not completely understood. The absence of activating *FcγRs*, *FcγRI*, *FcγRIII* or *FcγRIV* did not affect osteoclast differentiation and bone homeostasis at steady state⁹. No differences in cancellous bone volume, trabecular number, trabecular thickness, trabecular separation, or osteoclast number were observed among strains of knockouts. The role of *FcγRI*, *FcγRIII*, and *FcγRIV* on bone resorption during inflammatory arthritis was investigated. Lack of *FcγRIII* attenuated arthritis development and decreased inflammatory infiltration and cartilage destruction whereas deletion of *FcγRI* had no effect on arthritis after transfer of K/BxN serum²⁰. *FcγRIV*-deficient mice had a smaller area of inflammatory infiltrate and bone erosion⁹.

Our studies indicated that the inactivation of *FcγRIIB* resulted in cancellous osteopenia due to increased osteoclastic bone resorption following SLE development at 6 months of age. These data coincided with the lower lumbar spine and hip BMD in patients with SLE^{15,21}. Ten-month-old *FcγRIIB*^{-/-} mice had a substantial reduction

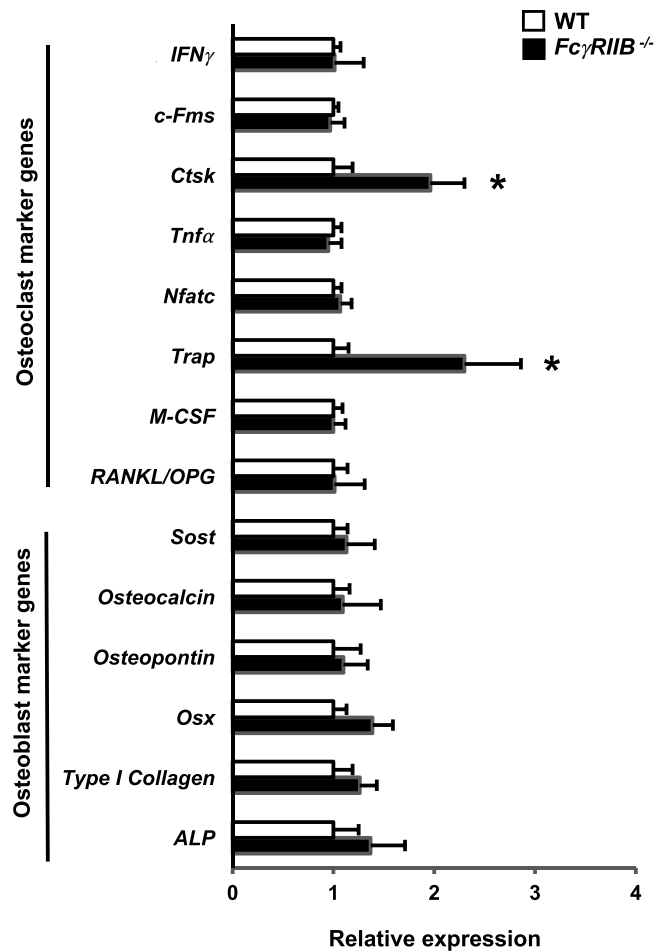


Figure 5. Absence of *FcγRIIB* upregulates osteoclast marker gene expression. qRT-PCR analysis of mRNA expression in the distal femur metaphysis from 10-month-old *FcγRIIB*^{-/-} males. Results are mean ± SEM. **p* < 0.05 versus WT controls.

in cancellous bone volume compared to younger mice, suggesting more severe bone loss with longer SLE disease duration. It has been reported that the inhibitory effect of *FcγRIIB* on osteoclast differentiation was mediated through IgGs²². IgG1 has a higher affinity for *FcγRIIB* and exhibits the strongest level of *FcγRIIB*-induced negative regulation³. The level of IgGs in *FcγRIIB*^{-/-} mice increased with age²². It is possible that the IgGs produced in *FcγRIIB*^{-/-} mice induces proinflammatory response during autoimmune disease, leading to cancellous bone loss.

Although the relationship between inflammatory cytokines and bone loss in patients with SLE remains unclear, increased osteoclast differentiation induced by proinflammatory cytokines is thought to be the cause of bone resorption in these patients. The inhibitory *FcγRIIB* is expressed on mast cells and macrophages which have the capacity to trigger strong proinflammatory responses. Patients with SLE are unable to perform IC clearance. These ICs can induce the production of cytokines, including IL-6, TNF-α and IL-10 by macrophages and dendritic cells^{23,24}. Enhanced production of TNF-α in 6- and 10-month-old *FcγRIIB*^{-/-} mice in our study coincides with the high serum level of TNF-α in the patients with active SLE disease²⁵. However, serum IL-6 and IL-10 levels were unaltered. The role of *FcγRIIB* in the release of proinflammatory mediator was demonstrated by enhanced macrophage responses in *FcγRIIB*^{-/-} mice with collagen-induced arthritis and IC-mediated alveolitis models^{11,26}. TNF-α antagonist, etanercept, is widely used for the treatment of inflammatory diseases, including rheumatoid arthritis, axial spondyloarthritis, psoriatic arthritis, and plaque psoriasis²⁷. Our study indicated that etanercept rescued the skeletal phenotype of *FcγRIIB*^{-/-} mice, indicating that TNF-α played a major role in cortical and cancellous bone loss in these mice.

MRL/lpr and BXSB/MpJ-Yaa mice are promising models of osteoporosis in murine lupus. It was found that MRL/lpr mice were osteopenic due to decreased bone formation²⁸. The BXSB/MpJ-Yaa mice have Yaa mutation on Y chromosome, and male mice therefore develop severe SLE disease. Three months old BXSB/MpJ-Yaa males had a normal skeletal phenotype²⁹. But osteopenia developed at 6 months of age. TRAP positive osteoclasts were increased without any change in osteocalcin positive cells, indicating increased bone resorption with normal bone formation. MRL/lpr mice have biphasic increase in circulating level and renal expression of TNF-α³⁰. The serum TNF-α level was peak in neonatal mice, normalized by 2 months of age and continuously increased again afterward. The renal TNF-α expression was detected in neonatal mice and dramatically decreased within 2 weeks. However, the expression was increased with progressive lupus nephritis in aged mice.

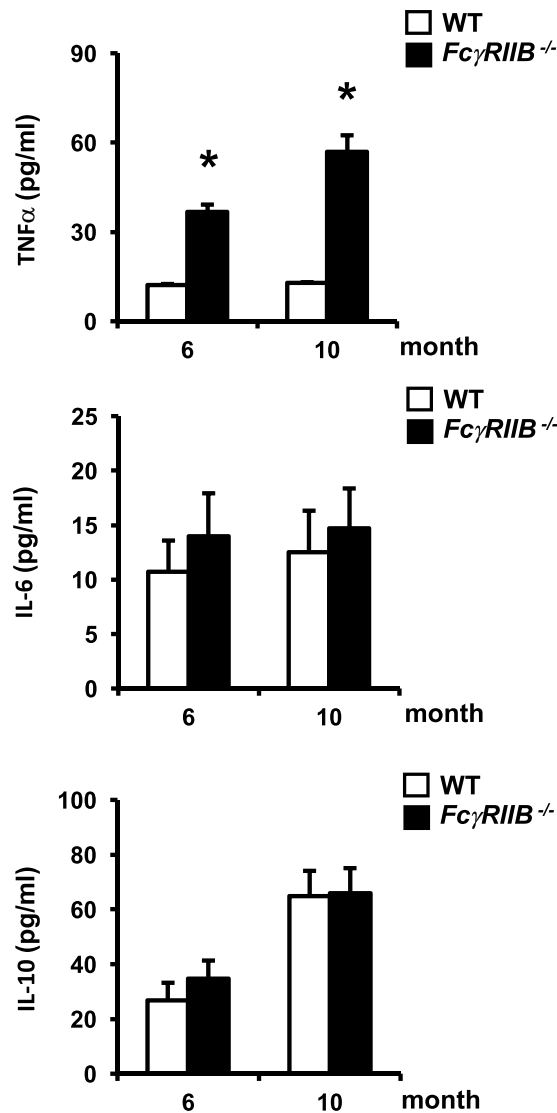


Figure 6. *FcγRIIB*^{-/-} mice had high serum levels of TNF-α. Serum levels of TNF-α, IL-6, and IL-10 in 6- and 10-month-old *FcγRIIB*^{-/-} males. Results are mean ± SEM. **p* < 0.05 versus corresponding WT controls.

Deleting *FcγRIIB* increased *Ctsk* and *Trap* mRNA expression, suggesting elevated bone resorption. In addition to *Ctsk*'s known function in osteoclasts, *Ctsk* may stimulate bone resorption through immune cell-mediated osteoclast activation. *Ctsk* deficiency reduced the proinflammatory cytokine expression in rheumatoid arthritis³¹. *Trap* is essential for skeletal development, bone mineralization, collagen metabolism, and cytokine production by dendritic cells and macrophages. Mice lacking *Trap* had an osteopetrotic phenotype, reduced resorptive activity during endochondral ossification, premature mineralization of epiphyseal cartilage, and shortened bones³².

Taken together, this study establishes the role of *FcγRIIB* on cancellous bone homeostasis as a link between SLE disease and osteoclast formation. Absence of *FcγRIIB* induces inflammation by enhancing TNF-α and increases osteoclastic bone resorption, resulting in cancellous bone loss in mice with active SLE disease. Therefore, *FcγRIIB* is an important candidate as a therapeutic target for autoimmune diseases and osteoporosis.

Materials and Methods

Experimental design. Male *FcγRIIB*^{-/-} mice on C57BL/6 background provided by Dr. Silvia Bolland (NIAID, NIH, Maryland, USA) were housed at the Faculty of Medicine, Chulalongkorn University. The experimental protocol was approved by the Institutional Animal Care and Use Committee at the Faculty of Medicine, Chulalongkorn University in accordance with the Guide for the Care and Use of Laboratory Animals (eighth edition), National Research Council. The mice were maintained at room temperature and housed on a 12 h light and 12 h dark cycle during the study. Standard mouse chow (C.P. Mice Feed, Perfect Companion Group Co., Ltd., Thailand) and water were provided *ad libitum* to all mice. Male *FcγRIIB*^{-/-} mice were crossed with C57BL/6 females purchased from the National Laboratory Animal Center, Mahidol University, Thailand to generate heterozygotes. Male and female *FcγRIIB*^{+/-} mice were crossed to obtain *FcγRIIB*^{+/-}, *FcγRIIB*^{-/-}, and wild type (WT)

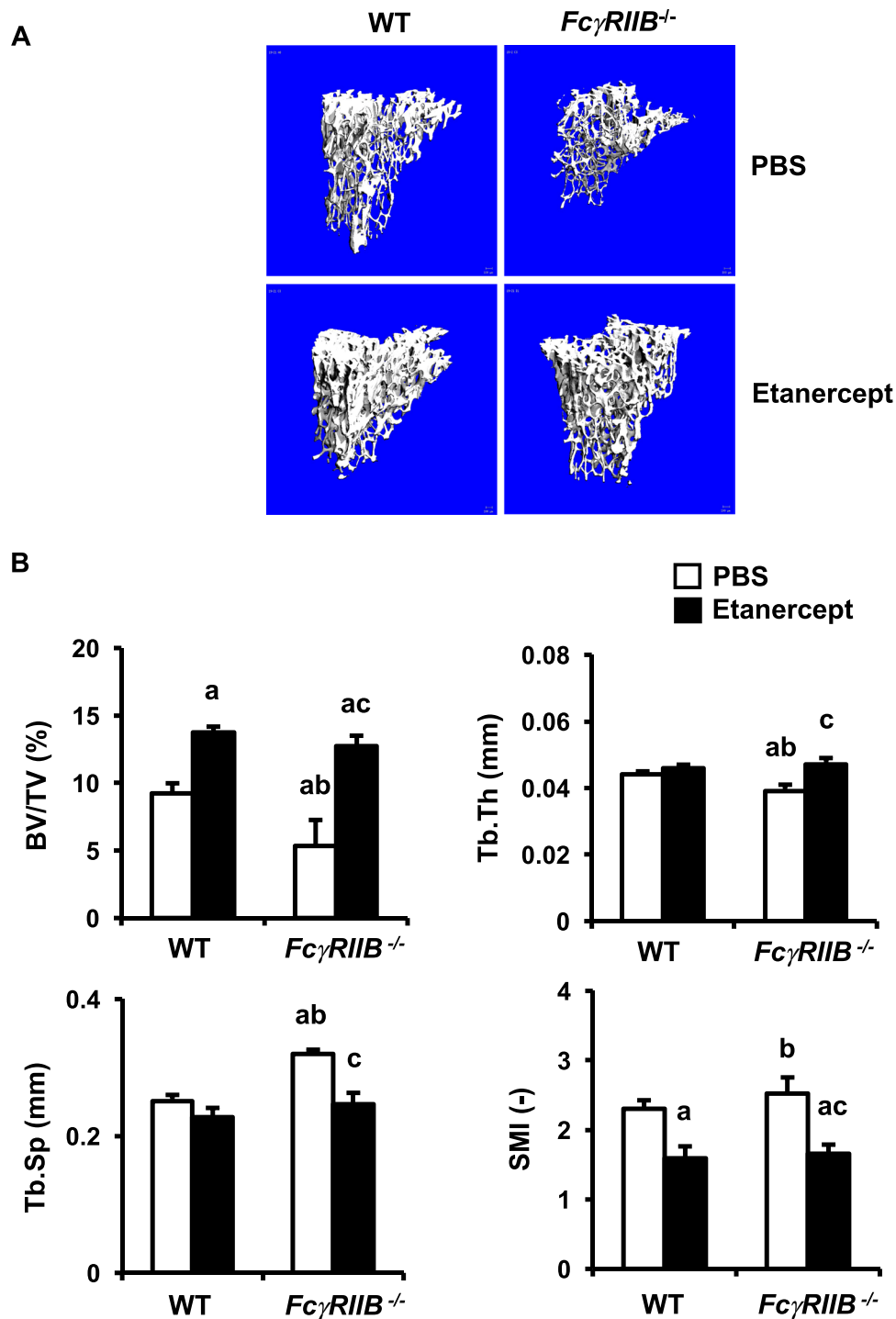


Figure 7. Blocking TNF- α prevents cancellous bone loss in *FcγRIIB*^{-/-} mice. (A) Representative μ CT images of the tibial cancellous bone from WT and *FcγRIIB*^{-/-} males treated with either PBS or etanercept. (B) μ CT analysis of the proximal tibial metaphysis. Results are mean \pm SEM. ^a $p < 0.05$ versus WT controls treated with PBS, ^b $p < 0.05$ versus WT controls treated with etanercept, and ^c $p < 0.05$ versus *FcγRIIB*^{-/-} mice treated with PBS.

control mice. The mice were genotyped using PCR (95 °C for 15 s, 60 °C for 30 s, and 72 °C for 30 s for 35 cycles) using 3 primers: 5'-AAGGCTGTGGTCAAACCTCGAGCC-3', 5'-CTCGTGCTTTACGGTATCGCC-3' and 5'-TTGACTGTGGCCTTAAACGTGTAG-3'.

The mice received double fluorochrome labeling with 20 mg/kg calcein (Sigma, St. Louis, MO, USA) to label mineralizing bone. The interlabel periods were 7 and 8 days for 6 and 10 months old *FcγRIIB*^{-/-} mice and WT controls, respectively. Three-, 6- and 10 months old mice were anesthetized with isoflurane and sacrificed by cervical dislocation. The left tibiae and femurs were fixed in 70% alcohol for microcomputed tomography (μ CT) and

histomorphometric analyses, respectively. The right femurs were removed and kept at -80°C for RNA isolation and qPCR analysis.

For TNF- α inhibitor administration, 6 months old *Fc γ RIIB $^{-/-}$* males and their WT controls were subcutaneously injected with either PBS or 25 mg/kg etanercept (Wyeth, New Jersey, USA) twice a week for 8 weeks. This dose is an intermediate dose for mice³³. At the end of experiment, left tibiae were removed and fixed in 70% alcohol for μ CT analysis

μ CT analysis. μ CT was used for nondestructive 3-dimensional evaluation of the bone microarchitecture using a μ CT35 scanner (Scanco Medical AG, Bassersdorf, Switzerland) according to standard guidelines³⁴. This technique quantitatively assesses cancellous and cortical bone morphology which provides information about the amount of bone. The bone samples were scanned at a voxel size of $7\ \mu\text{m}$, 50 kVp, $144\ \mu\text{A}$ and 800 ms integration time. The machine was set at a threshold of 220 to distinguish bone from soft tissues. Four hundred and sixty four transverse slices of the cancellous bone at the proximal tibial metaphysis were scanned. Cancellous bone was assessed in 300 transverse slices to determine bone volume (BV/TV, %), trabecular thickness (Tb.Th, mm), trabecular number (Tb.N, /mm), trabecular separation (Tb.Sp, mm), and structural model index (SMI, -).

Histomorphometry. The left femurs were dehydrated in graded acetone, infiltrated and embedded undecalcified in methyl methacrylate. Longitudinal sections ($4\ \mu\text{m}$ thick) were cut with a microtome (Leica 2065). A section was left unstained for determining the dynamic parameters including mineralizing surface per bone surface (MS/BS, %), mineral apposition rate (MAR, $\mu\text{m}/\text{day}$), and bone formation rate adjusted for bone surface (BFR/BS, $\mu\text{m}^3/\mu\text{m}^2/\text{year}$), bone volume (BFR/BV, %/year) and tissue volume (BFR/TV, %/year). A consecutive section was stained with toluidine blue for cell-based measurements, including osteoblast surface per bone surface (Ob.S/BS, %), osteoblast number per bone perimeter (N.Ob/B.Pm, /mm), osteoblast number per tissue area (N.Ob/T.Ar, /mm²), osteoid thickness (O.Th, μm), osteoid surface per bone surface (OS/BS, %), osteoid volume per tissue volume (OV/TV, %), osteoclast surface per bone surface (Oc.S/BS, %), osteoclast number per bone perimeter (N.Oc/B.Pm, /mm), osteoclast number per tissue area (N.Oc/T.Ar, /mm²), and eroded surface per bone surface (ES/BS, %). Histomorphometric data were obtained using the OsteoMeasure System (OsteoMetrics, Inc., Atlanta, GA, USA). All parameters were reported using standardized nomenclature³⁵.

Osteoblast differentiation. Primary osteoblasts derived from the long bones of *Fc γ RIIB $^{-/-}$* males and their control littermates were prepared as previously described³⁶. The cells were cultured in differentiation medium containing α -MEM supplemented with 10% FBS, 100 unit/ml penicillin and 100 $\mu\text{g}/\text{ml}$ streptomycin, 10 μM dexamethasone, 5 mM β -glycerophosphate, and 50 $\mu\text{g}/\text{ml}$ ascorbic acid. Osteoblasts were fixed with 3.7% formaldehyde, and stained for ALP and mineralized bone nodules with Fast Blue RR (Sigma, St. Louis, MO, USA), and 2% alizarin red (Sigma, St. Louis, MO, USA) on days 7 and 21, respectively. ALP activity was quantified as previously described³⁷. Mineralization was measured by extraction of calcified mineral stained with alizarin red using 10% cetylpyridinium chloride in 10 mM sodium phosphate (pH 7)³⁶. The concentration of alizarin red (mM) after destaining was determined.

Osteoclast differentiation. Bone marrow cells were cultured in α -MEM containing 10% FBS, 100 unit/ml penicillin and 100 $\mu\text{g}/\text{ml}$ streptomycin for 24 h to obtain BMMs. The BMMs were then cultured on coverslips in α -MEM containing 20 ng/ml M-CSF (R&D Systems, Inc., MN, USA) for 2 days and in the same medium containing 20 ng/ml M-CSF, and 3.3 ng/ml RANKL (R&D Systems, Inc., MN, USA) for an additional 6 days. TRAP-positive spreading osteoclasts containing more than 5 nuclei were quantified using OsteoMeasure software.

For co-culture studies, osteoblasts derived from the long bones of *Fc γ RIIB $^{-/-}$* males and their WT controls were cultured in α -MEM containing 10% FBS, 100 unit/ml penicillin and 100 $\mu\text{g}/\text{ml}$ streptomycin for 24 h. BMMs from either *Fc γ RIIB $^{-/-}$* mice or WT controls were added and cultured in α -MEM containing 10^{-6} M prostaglandin E₂ (Merck Millipore, Burlington, MA, USA) and 10^{-8} M 1,25-dihydroxyvitamin D₃ (Merck Millipore, Burlington, MA, USA) for 4 days. TRAP-positive spreading osteoclasts containing more than 5 nuclei were counted using OsteoMeasure software.

qPCR analysis. The right femur distal metaphyses were pulverized in liquid nitrogen. Total RNA was isolated using Trizol reagent (Invitrogen, Carlsbad, CA, USA) according to the manufacturer's protocol. The samples were purified using an RNeasy Mini kit (Qiagen, Hilden, Germany). cDNA was synthesized using SuperScript VILO (Invitrogen, Carlsbad, CA, USA). The qPCR was performed at 60°C for 40 cycles using CFX96™ Optics Module (Bio-Rad, CA, USA) and GAPDH was used as an internal control for quantification. The primer sequences are listed in Supplementary Table S1.

Serum cytokines. Serum cytokines, TNF- α , IL-6, and IL-10 were measured by ELISA according to the manufacturer's protocol (ThermoFisher Scientific, Waltham, MA, USA).

Statistical analysis. All data are expressed as mean \pm SEM. The unpaired Student's t-test was used to compare the differences between 2 groups. The significance of differences between 3 groups was analyzed using one-way ANOVA followed by Fisher's protected least significant difference test. Interactions between *Fc γ RIIB* deletion and etanercept were determined by two-way ANOVA. Differences were defined as significant at $p < 0.05$.

Data availability

All data are available from the corresponding author upon request.

Received: 29 October 2018; Accepted: 7 November 2019;

Published online: 22 November 2019

References

- Bultink, I. E. M. Bone Disease in Connective Tissue Disease/Systemic Lupus Erythematosus. *Calcified tissue international* **102**, 575–591, <https://doi.org/10.1007/s00223-017-0322-z> (2018).
- Tang, X. L. *et al.* SLE disease per se contributes to deterioration in bone mineral density, microstructure and bone strength. *Lupus* **22**, 1162–1168, <https://doi.org/10.1177/0961203313498802> (2013).
- Nimmerjahn, F. & Ravetch, J. V. Fcγ receptors as regulators of immune responses. *Nature reviews. Immunology* **8**, 34–47, <https://doi.org/10.1038/nri2206> (2008).
- Takai, T., Ono, M., Hikida, M., Ohmori, H. & Ravetch, J. V. Augmented humoral and anaphylactic responses in Fcγ RII-deficient mice. *Nature* **379**, 346–349, <https://doi.org/10.1038/379346a0> (1996).
- Smith, K. G. & Clatworthy, M. R. Fcγ RIIb in autoimmunity and infection: evolutionary and therapeutic implications. *Nat Rev Immunol* **10**, 328–343, <https://doi.org/10.1038/nri2762> (2010).
- Uher, F., Lamers, M. C. & Dickler, H. B. Antigen-antibody complexes bound to B-lymphocyte Fcγ receptors regulate B-lymphocyte differentiation. *Cellular Immunology* **95**, 368–379 (1985).
- Bolland, S. & Ravetch, J. V. Spontaneous autoimmune disease in Fc(γ)RIIb-deficient mice results from strain-specific epistasis. *Immunity* **13**, 277–285 (2000).
- McGaha, T. L., Sorrentino, B. & Ravetch, J. V. Restoration of tolerance in lupus by targeted inhibitory receptor expression. *Science* **307**, 590–593, <https://doi.org/10.1126/science.1105160> (2005).
- Seeling, M. *et al.* Inflammatory monocytes and Fcγ receptor IV on osteoclasts are critical for bone destruction during inflammatory arthritis in mice. *Proceedings of the National Academy of Sciences of the United States of America* **110**, 10729–10734, <https://doi.org/10.1073/pnas.1301001110> (2013).
- van Lent, P. L. *et al.* Fcγ receptors directly mediate cartilage, but not bone, destruction in murine antigen-induced arthritis: uncoupling of cartilage damage from bone erosion and joint inflammation. *Arthritis Rheum* **54**, 3868–3877, <https://doi.org/10.1002/art.22253> (2006).
- Yuasa, T. *et al.* Deletion of fcgamma receptor IIB renders H-2(b) mice susceptible to collagen-induced arthritis. *The Journal of experimental medicine* **189**, 187–194 (1999).
- Saiworn, W. *et al.* Cortical Bone Loss in a Spontaneous Murine Model of Systemic Lupus Erythematosus. *Calcified tissue international*. <https://doi.org/10.1007/s00223-018-0464-7> (2018).
- Amarasekara, D. S., Yu, J. & Rho, J. Bone Loss Triggered by the Cytokine Network in Inflammatory Autoimmune Diseases. *Journal of immunology research* **2015**, 832127, <https://doi.org/10.1155/2015/832127> (2015).
- Tang, Y. *et al.* Activated NF-κB in bone marrow mesenchymal stem cells from systemic lupus erythematosus patients inhibits osteogenic differentiation through downregulating Smad signaling. *Stem cells and development* **22**, 668–678, <https://doi.org/10.1089/scd.2012.0226> (2013).
- Teichmann, J., Lange, U., Stracke, H., Federlin, K. & Bretzel, R. G. Bone metabolism and bone mineral density of systemic lupus erythematosus at the time of diagnosis. *Rheumatol Int* **18**, 137–140 (1999).
- Gergely, P. Jr. *et al.* Altered expression of Fcγ and complement receptors on B cells in systemic lupus erythematosus. *Ann N Y Acad Sci* **1108**, 183–192 (2007).
- Floto, R. A. *et al.* Loss of function of a lupus-associated FcγRIIb polymorphism through exclusion from lipid rafts. *Nat Med* **11**, 1056–1058, <https://doi.org/10.1038/nm1288> (2005).
- Kleinau, S., Martinsson, P. & Heyman, B. Induction and suppression of collagen-induced arthritis is dependent on distinct fcgamma receptors. *The Journal of experimental medicine* **191**, 1611–1616 (2000).
- Koga, T. *et al.* Costimulatory signals mediated by the ITAM motif cooperate with RANKL for bone homeostasis. *Nature* **428**, 758–763, <https://doi.org/10.1038/nature02444> (2004).
- Ji, H. *et al.* Arthritis critically dependent on innate immune system players. *Immunity* **16**, 157–168 (2002).
- Bultink, I. E. Osteoporosis and fractures in systemic lupus erythematosus. *Arthritis Care Res (Hoboken)* **64**, 2–8, <https://doi.org/10.1002/acr.20568> (2012).
- Negishi-Koga, T. *et al.* Immune complexes regulate bone metabolism through Fcγ signaling. *Nat Commun* **6**, 6637, <https://doi.org/10.1038/ncomms7637> (2015).
- Radstake, T. R. *et al.* Increased FcγRII expression and aberrant tumour necrosis factor alpha production by mature dendritic cells from patients with active rheumatoid arthritis. *Ann Rheum Dis* **63**, 1556–1563, <https://doi.org/10.1136/ard.2003.016550> (2004).
- Ronnelid, J., Tejde, A., Mathsson, L., Nilsson-Ekdahl, K. & Nilsson, B. Immune complexes from SLE sera induce IL10 production from normal peripheral blood mononuclear cells by an FcγRII dependent mechanism: implications for a possible vicious cycle maintaining B cell hyperactivity in SLE. *Ann Rheum Dis* **62**, 37–42 (2003).
- Davis, L. S., Hutcheson, J. & Mohan, C. The role of cytokines in the pathogenesis and treatment of systemic lupus erythematosus. *J Interferon Cytokine Res* **31**, 781–789, <https://doi.org/10.1089/jir.2011.0047> (2011).
- Clynes, R. *et al.* Modulation of immune complex-induced inflammation *in vivo* by the coordinate expression of activation and inhibitory Fc receptors. *The Journal of experimental medicine* **189**, 179–185 (1999).
- Burness, C. B. & Duggan, S. T. Etanercept (SB4): A Review in Autoimmune Inflammatory Diseases. *BioDrugs* **30**, 371–378, <https://doi.org/10.1007/s40259-016-0188-z> (2016).
- Shapira, D., Kabala, A., Raz, B. & Israeli, E. Osteoporosis in murine systemic lupus erythematosus—a laboratory model. *Lupus* **10**, 431–438, <https://doi.org/10.1191/096120301678646182> (2001).
- Namba, T. *et al.* Feature Article: Altered morpho-functional features of bones in autoimmune disease-prone BXSB/MpJ- Yaa mice. *Exp Biol Med (Maywood)* **244**, 333–343, <https://doi.org/10.1177/1535370219832810> (2019).
- Yokoyama, H., Kreft, B. & Kelley, V. R. Biphasic increase in circulating and renal TNF-α in MRL-lpr mice with differing regulatory mechanisms. *Kidney Int* **47**, 122–130, <https://doi.org/10.1038/ki.1995.14> (1995).
- Hao, L. *et al.* Deficiency of cathepsin K prevents inflammation and bone erosion in rheumatoid arthritis and periodontitis and reveals its shared osteoimmune role. *FEBS Lett* **589**, 1331–1339, <https://doi.org/10.1016/j.febslet.2015.04.008> (2015).
- Blumer, M. J. *et al.* Role of tartrate-resistant acid phosphatase (TRAP) in long bone development. *Mech Dev* **129**, 162–176, <https://doi.org/10.1016/j.mod.2012.04.003> (2012).
- Yoshitaka, T. *et al.* Etanercept administration to neonatal SH3BP2 knock-in cherubism mice prevents TNF-α-induced inflammation and bone loss. *Journal of bone and mineral research: the official journal of the American Society for Bone and Mineral Research* **29**, 1170–1182, <https://doi.org/10.1002/jbmr.2125> (2014).
- Bouxein, M. L. *et al.* Guidelines for assessment of bone microstructure in rodents using micro-computed tomography. *Journal of bone and mineral research: the official journal of the American Society for Bone and Mineral Research* **25**, 1468–1486, <https://doi.org/10.1002/jbmr.141> (2010).
- Dempster, D. W. *et al.* Standardized nomenclature, symbols, and units for bone histomorphometry: a 2012 update of the report of the ASBMR Histomorphometry Nomenclature Committee. *Journal of bone and mineral research: the official journal of the American Society for Bone and Mineral Research* **28**, 2–17, <https://doi.org/10.1002/jbmr.1805> (2013).

36. Lotinun, S. *et al.* Osteoclast-specific cathepsin K deletion stimulates S1P-dependent bone formation. *The Journal of clinical investigation* **123**, 666–681, <https://doi.org/10.1172/JCI64840> (2013).
37. Addison, W. N. & McKee, M. D. Inositol hexakisphosphate inhibits mineralization of MC3T3-E1 osteoblast cultures. *Bone* **46**, 1100–1107, <https://doi.org/10.1016/j.bone.2010.01.367> (2010).

Acknowledgements

We thank Dr. Kevin Tompkins for his careful reading of the manuscript and helpful suggestions. This work was supported by the Ratchadapisek Sompoch Endowment Fund (2014), Chulalongkorn University (CU-57-091-IC), and the Faculty of Dentistry, Chulalongkorn University (DRF 61019) to S. Lotinun.

Author contributions

P.V., W.S. and P.J. performed the experiments and acquired data. A.L. and P.P. discussed the results and provided some suggestion. S.L. designed and performed the experiments, analyzed data, and wrote the manuscript. All authors revised the manuscript and approved the final version of the manuscript.

Competing interests

The authors declare no competing interests.

Additional information

Supplementary information is available for this paper at <https://doi.org/10.1038/s41598-019-53963-z>.

Correspondence and requests for materials should be addressed to S.L.

Reprints and permissions information is available at www.nature.com/reprints.

Publisher's note Springer Nature remains neutral with regard to jurisdictional claims in published maps and institutional affiliations.



Open Access This article is licensed under a Creative Commons Attribution 4.0 International License, which permits use, sharing, adaptation, distribution and reproduction in any medium or format, as long as you give appropriate credit to the original author(s) and the source, provide a link to the Creative Commons license, and indicate if changes were made. The images or other third party material in this article are included in the article's Creative Commons license, unless indicated otherwise in a credit line to the material. If material is not included in the article's Creative Commons license and your intended use is not permitted by statutory regulation or exceeds the permitted use, you will need to obtain permission directly from the copyright holder. To view a copy of this license, visit <http://creativecommons.org/licenses/by/4.0/>.

© The Author(s) 2019